Effect of combined dilute-alkaline and green pretreatments on corncob fractionation: Pretreated biomass characterization and regenerated cellulose film production

David Araújo [a,b,*], Maria Vilarinho [b,c], Ana Machado [a]

[a] Institute for Polymers and Composites/i3N, University of Minho, Guimarães, Portugal

[b] Centre for Waste Valorization, University of Minho, Guimarães, Portugal

[c] Mechanical Engineering and Resources Sustainability Centre, University of Minho, Guimarães, Portugal

Keywords:

Lignocellulosic biomass
Green pretreatments
Regenerated film
Cellulose
Crystallinity
Thermal stability

Abstract

Pretreatment is an essential step prior to the effective valorization of lignocellulosic biomass. However, depending on the pretreatment method, it can be costly and originate potential environmental threats. In this study, green pretreatments, namely Liquid Hot Water (LHW) and 1-butyl-3-methylimidazolium chloride (BmimCl), as well as low concentrated sodium hydroxide solution (NaOH), were applied individually and in combination to pretreat corncob, and their effects on physicochemical properties of fibers were analyzed. The pretreated samples were dissolved in ionic liquid and attempts to prepare regenerated cellulose films have been made. While NaOH was

efficient to removal lignin, LHW presented higher solubilization hemicellulose. By combining these treatments, the biomass was fractionated in a complementary way, and a solid enrich-cellulose fraction with high thermal stability and crystallinity was obtained. The BmimCl did not significantly change the chemical composition of biomass and, independent of the treatment applied in combination, samples were regenerated as amorphous cellulose coexisting with lesser amount of cellulose crystalline I. This structural conversion was also confirmed through thermogravimetric analysis, from which a decrease in thermal stability was verified. This latter property was markedly affected by the presence of hemicellulose remained after some pretreatments. The obtained results indicate that each pretreatment performed can meet different application requirements. The LHW-NaOH pretreated sample was the only one suitable to produce regenerated films, which exhibited good mechanical properties to be used in value-added applications, such as packaging.

Introduction

The depletion of fossil resources, as well as the social and environmental impacts associated with its extraction and production chain, have fostered, in recent years, the search for unconventional and renewable substitute raw materials. Among the available sources, lignocellulosic biomass (LCB) has been extensively studied and has shown potential to be applied as a starting substrate to produce value-added materials, such as biofuels and biopolymers (Brodin et al., 2017; Ravindran and Jaiswal, 2016; Reddy and Rhim, 2014; Zhou et al., 2018). Its abundant availability and accessibility make the LCB a source of easy acquisition and low cost, but still underexploited (Araújo et al., 2018). For instance, Corncob is an agroindustrial residue widely generated and little valued. To date, corncobs are used on a limited basis for bedding, animal feed, oil sorbent and polishing agent (Araújo et al., 2018; Silvério et al., 2013). In Brazil it is estimated an average generation of more than 18,000 kilotons per year, of which 2990 kilotons would be available (Araújo et al., 2018).

LCB is essentially composed of natural biopolymers (cellulose, hemicellulose and lignin) and its main sources include agroindustrial residues, forest residues and municipal and industrial waste (Ullah et al., 2015). The main drawback regarding the valorization of LCB deals with the presence of covalent crosslinks between cellulose and hemicellulose with lignin in the cell wall of plants, which leads to its recalcitrant property. Hence, in order to disrupt this complex structural arrangement, pretreatments are usually performed prior to its effective use and valorization.

The application of pretreatment techniques basically promotes the disruption and fractionation of LCB components, which opens the material structure and facilitates the performance of subsequent processes (Bhutto et al., 2017; Seidl and Goulart, 2016). When it turns to added value cellulose-based biopolymeric materials production, the

application of pretreatments aiming the selective delignification of biomass to obtain a solid cellulose enriched fraction is of crucial importance. Otherwise, the presence of substantial amounts of non-cellulosic materials on fibers may negatively influence their structure and properties (Abdulkhani et al., 2013; Reddy and Yang, 2005; Sánchez, 2009).

Basically, the pretreatments methods can be classified into four categories, namely physical, chemical, physicochemical and biological. Some of the existing and applicable

methods make use of harsh chemicals and severe treatment conditions (Capolupo and Faraco, 2016). However, as the use of cellulose extracted from renewable raw materials is mainly motivated by its environmentally-friendly concept, it does not make sense to adopt non-sustainable processing techniques. Therefore, more recent studies within this scope have been aimed at optimizing the so-called green pretreatment technologies in order to develop less costly and environmentally harmful processes (Capolupo and Faraco, 2016; Daza Serna et al., 2016; Singh et al., 2016; Zhang et al., 2017). In addition, since the performance and efficiency of each pretreatment varies widely according to its reaction mechanisms and the chemical and structural characteristic of biomass, the optimization of a single pretreatment is not always the universal choice for a specific purpose (Capolupo and Faraco, 2016; Chen et al., 2017). Thus, to overcome possible drawbacks associated with single operations, such as technological problems, high-energy consumption and long reaction times, combined processes have been extensively applied. Generally, their application can significantly improve the synergistic aspects involved in the treatment of biomass, which can lead, for example, to better performance of delignification (Chen et al., 2017; Zhang et al., 2017).

Liquid hot water (LHW) and room temperatures ionic liquids (IL), in response to their fractionation efficiency and eco-friendly aspect, are among the main green pretreatment methods applied to fractionate biomass. Regarding the conventional techniques, NaOH pretreatment is the most widely chemical pretreatment used, mainly because of its simplified application and excellent delignification capacity. NaOH solutions essentially cause the cleavage of intermolecular α - and β-aryl ether linkages between hemicellulose and lignin, leading to a swelling of the biomass pores, disruption of the lignin structure and an increase of available surface area (Chen et al., 2017; Rabemanolontsoa and Saka, 2016; Sun and Cheng, 2002; Yue et al., 2015). This alkaline treatment is one of the preferred pretreatment technologies since it is carried out under mild conditions, does not present physical hazard (explosive, combustible and oxidizing), does not have sufficient volatility to constitute an inhalation danger, besides being non-carcinogenic, non-persistent and non-bioaccumulative (Government of Canada, 2017; Kim et al., 2016; Wan et al., 2011). In addition, the direct contact with NaOH solutions should be prevented only for concentrations higher than 2% (in water), due to its corrosive effects (Hellenic Petroleum, 2013). The main downsides related to this pretreatment deals with the processing time and the black liquor generated. These problems can be partially mitigated by using the NaOH technique in combination with other treatments, which ultimately demands low concentrated solutions and reduced processing times (Chen et al., 2013). Notwithstanding, it is worth to emphasize that the black liquor has yet to be treated even after dilute-alkaline treatment, and its economically and environmentally feasibility must be taken into account when planning large scale plants.

Liquid Hot Water is a physicochemical or hydrothermal method that uses only water at reasonably milder conditions compared to other pretreatments. During the process, water penetrates into the biomass structure and substantially hydrolyze hemicelluloses (up to 80%) and partially removes lignin (Agbor et al., 2011; Capolupo and Faraco, 2016; Michelin and Teixeira, 2016; Rabemanolontsoa and Saka, 2016; Sabanci and Buyukkileci, 2018). The chemical effect in the LHW occurs as an autohydrolysis process since the organic acids released from polysaccharides auto-catalyze the hydrolysis of hemicellulose and lignin. The main advantages of this method comprise low environmental impact, low cost and the no need of chemicals or catalysts. Ionic Liquids are salts with low melting point ($< 100^{\circ}C$) composed by organic cations and organic or inorganic anions. The application of ionic liquids in chemical reactions is considered a

green method due to its characteristics, namely thermal stability, inflammability, low volatility and recyclability (Brandt et al., 2013; Farrán et al., 2015; Lopes et al., 2017). Ionic liquids constituted by imidazolium cations, such as 1-allyl-3-methylimidazolium and 1-butyl-3-methylimidazolium chloride, are the most applied to biomass fractionation and cellulose dissolution (Brandt et al., 2013). In this process, firstly the ionic liquid anions are able to form hydrogen bonds with hydroxyl groups of biomass, leading to its structural disruption and dissolution. Subsequently, the cellulose fraction can be recovered as a regenerated product by addition of organic solvents. The successful dissolution of lignocellulosic biomass in BmimCl was demonstrated by Fort et al. (2007), Kilpeläinen et al.(2007) and Pang et al. (2016).

Within the scope of cellulose-based materials produced from LCB, regenerated cellulose films synthesized from green and non-derivatizing solvents (such as ionic liquids) have drawn increasing attention as they possess excellent physical and chemical properties, and also because the dissolution and regeneration techniques are simple, sustainable, versatile and easy for industrialization (Wang et al., 2016). Regenerated films prepared from others LCB through dissolution in IL have shown remarkable mechanical properties, besides transparency and non-toxicity, which gives them great potential applications (Nor Amalini et al., 2017; Pang et al., 2015; Reddy et al., 2017; Zhang et al., 2019). However, the production of regenerated cellulose films requires cellulose-enriched samples with a very small percentage of other constituents (such as lignin and hemicellulose). In order to achieve this, standard methods of pulping and bleaching as pretreatments are still commonly used, which goes against the environmental sustainability imputed by the resources and techniques (dissolution and regeneration) applied.

The aim of this work is to investigate the effect of combined pretreatments, including green and dilute-alkaline techniques, on physicochemical properties of corncob fibers and prepare regenerated cellulose films from pretreated samples using BmimCl as a solvent. Combined pretreatments including chemical and physicochemical methods, namely dilute sodium hydroxide (NaOH), Liquid Hot Water (LWH) and Ionic Liquid (IL), were selected based on their complementary characteristics, and to the best of our knowledge, some combinations set in this paper have not yet been addressed for the treatment of corncob, namely LHW-dilute NaOH and LHW-BmimCl. In literature, studies performed in the scope of corncob fractionation by applying combined pretreatments can be found, whilst not exhaustive (Kawee-Ai et al., 2016; Luo et al., 2013; Michelin et al., 2018; Thangavelu et al., 2018; Upajak et al., 2018; Xie et al., 2014). It should be emphasized that the combined treatments proposed are designed as two and three-stage pretreatments. Besides being scalable and nonconflicting, this arrangement may avoid drawbacks such as the generation of sugar degradation by-products in certain combinations, as verified by Imman et al. (2015) and Yang et al. (2019) when NaOH was used as a catalyst in LHW treatment. The characterization of the physicochemical changes on pretreated samples and regenerated films was accomplished by compositional, morphological, X-Ray diffraction and Fourier transform infrared spectroscopy analysis, as well as by thermal characterization. Dynamic mechanical analysis of the regenerated cellulose films was also performed.

Materials and methods

Materials

Corncob (CC) was obtained from local agricultural cooperatives from the North of Portugal. The corncob residue was firstly ground and sieved to particles sizes from 0.25 to 0.5 mm and stored in sealed plastic bags at room temperature. Cellulose sheets (cellulose pulp), provided by a local factory, were torn into small fragments and dried at 60°C for 24 h . Ionic liquid 1-butyl-3-methylimidazolium chloride was purchased from Sigma-Aldrich (98%), Germany, and used as received. Sodium hydroxide (pellets) was acquired from Fisher Chemicals.

Liquid hot water treatment

Pretreatment was performed in a stainless steel cylindrical reactor (10 cm internal diameter and 24 cm internal height) with an approximate volume of 2 L . Feedstock loading rate of 10% (residue weight / distilled water volume) was pretreated at 190°C, 0.79MPa, for 30 min (after the heat-up time) under constant mechanical stirring. After the reactor was cooled by means of a coupled cooling system. The insoluble solid was collected, thoroughly washed with deionized water and dried at 60°C for further treatments and analysis (this sample was named as LWH-CC). The choice of the experimental conditions was based on the calculation of the severity factor $\left(\log\left(R_0\right)\right)$, which can be used as an indicator of the effects of destruction, disaggregation and depolymerization of biomass. The severity factor was calculated according to Eq. (1) (Heitz et al., 1991), that associate the residence time (t, min), the holding temperature (T, °C) and an empirical parameter (14.75) related to activation energy and temperature.

$$\log\left(\mathrm{R_0}\right) = \log\left[\exp\left(\frac{\mathrm{T}-100}{14.75}\right)\mathrm{t}\right] \quad (1)$$

Alkali treatment of corncob

Dried corncob and liquid hot water treated corncob (LHW - CC) were soaked in NaOH with 2wt.% concentration at 90°C for 1.5 h at a 1/30 solid/liquid ratio (w/w) under magnetic stirring. The alkali treated corncob (NaOH-CC) and LHW-CC (NaOH-LHW-CC) were then filtered and washed several times with deionized water until colorless. The resulting material was dried at 60°C for further treatments and characterization.

Ionic liquid treatment and regeneration of treated biomass

Prior to biomass dissolution, BmimCl was poured into a 100 mL beaker and thoroughly stirred at 100°C for 20 min in order to evaporate any residual moiety. After that, raw corncob, LHW-CC, NaOH-CC, NaOH -LHW-CC and cellulose pulp (CP) samples were dispersed, individually, in the ionic liquid at a 4% solid/liquid (w/w) ratio and treated at about 130°C under magnetic stirring for 5 h, 2 h, 1.5 h, 1.5 h and 0.5 h , respectively. The previously pretreated samples were kept under treatment in the ionic liquid until complete dissolution and a homogeneous solution was obtained. Particularly to the raw corncob residue, the treatment was undertaken under different dissolution times, ranging from 1 to 5 h , in order to verify the optimal treatment condition. However, even after 5 h of treatment the raw corncob did not dissolve completely.

After the treatment, the temperature was set to about 60°C and a mixture of acetone and ethanol, composed as a molar ratio X (acetone): Y (ethanol): Z (ionic liquid) with X =

3.5, Y = 1 and Z = 1, was added into the solution containing IL and biomass and stirred vigorously to precipitate the regenerated cellulosic biomass. The solid material precipitated was separated by vacuum filtration, washed 3-4 times with distilled water to remove residual ionic liquid and dried in an oven at 60°C for further treatments and analysis. The resulting BmimCl treated samples are referred to as IL-CC, IL-LWH-CC, IL-NaOH-CC and IL-NaOH − LHW − CC. A schematic arrangement of pretreatments performed is presented in Fig. 1.

Characterization of untreated and treated corncob

Thermogravimetric analysis and differential scanning calorimetry (DSC)

Thermogravimetry analyses and DSC of untreated and treated corncob were performed simultaneously on TA Instruments SDT 2960 model. The sample weight was in the range of 3 − 5mg and heated from 30 to 700°C at a rate of 10°C/min, under purified argon to prevent thermo-oxidative degradation.

Chemical composition of untreated and treated biomass

The chemical composition of all samples was determined by deconvolution of the derivative curves obtained from the thermogravimetry analysis (Carrier et al., 2011; Chen et al., 2016; Saldarriaga et al., 2015; Teng et al., 1997). The decomposition processes of the three pseudo-components presented in the lignocellulosic biomass (cellulose, hemicellulose and lignin) were modeled by a Gaussian distribution. For this, a multi-peaks method was used to determine the Gaussian distribution model using the Levenberg-Marquardt algorithm (the modeled equation, as well as graphs and parameters are available in the supplementary information). The percentage of each component was assumed to correspond to the integrated area above each single deconvoluted reaction curve.

Fourier transform infrared spectroscopy (FTIR)

FTIR spectra of cellulose, as well as treated and untreated biomass samples, were recorded on a Jasco FT/IR-4100 spectrometer. The ground and dried samples were pelletized with KBr and the spectra were obtained in the wavelength range $400 - 4000\ \text{cm}^{-1}$ at a resolution of $4\ \text{cm}^{-1}$.

X-Ray diffraction (XRD) analysis

The X-ray diffractograms patterns of all samples were obtained at room temperature using a diffractometer Bruker D8 Discover, operated with Cu-Ka radiation (wavelength of 0.154 nm) at a power of 40 mA and accelerating voltage of 40 kV . Diffraction intensities were scanned in the range of $2\theta = 5 - 50^{\circ}$ with a scanning rate of $0.05^{\circ}/$ second. The crystallinity index (Crl) of samples was determined by the Segal method (Segal et al., 1959) according to the following Eq. (2).

$$\text{Crl} = \left(\frac{I_{002} - I_{AM}}{I_{002}}\right) \times 100$$

Crl express the relative degree of crystallinity, I_{002} is the maximum intensity of the 002 lattice diffraction, found between the scattering angles of $2\theta = 22^{\circ}$ and 23°, and I_{AM} is the

minimum intensity, positioned between the 002 and 101 diffraction peaks (typically between $2\theta = 18^{\circ}$ and 19°). It is assumed that the I_{AM} have little crystalline contribution, comprising only the amorphous contribution, while the I_{002} represents both crystalline and amorphous regions.

Morphological analysis

The surface morphologies of untreated and treated samples were examined by scanning electron microscopy (SEM) using a FEI Nova 200. Samples were previously sputter coated with gold.

Preparation of regenerated cellulose film

To produce the cellulose films, a 4% (wt.) solution was prepared by dissolving 0.2 g of the extracted cellulose in 5 g of BmimCl under magnetic stirring at 120°C for 1.5 h . After completely dissolved, the regenerated film was made by solution casting on a glass plate using an alloy spreader, followed by soaking in 70 ml of deionized water. After 1 h the deionized water was replaced and left for another hour. Then, the regenerated cellulose film was dried at room temperature for 24 h in vacuum desiccator.

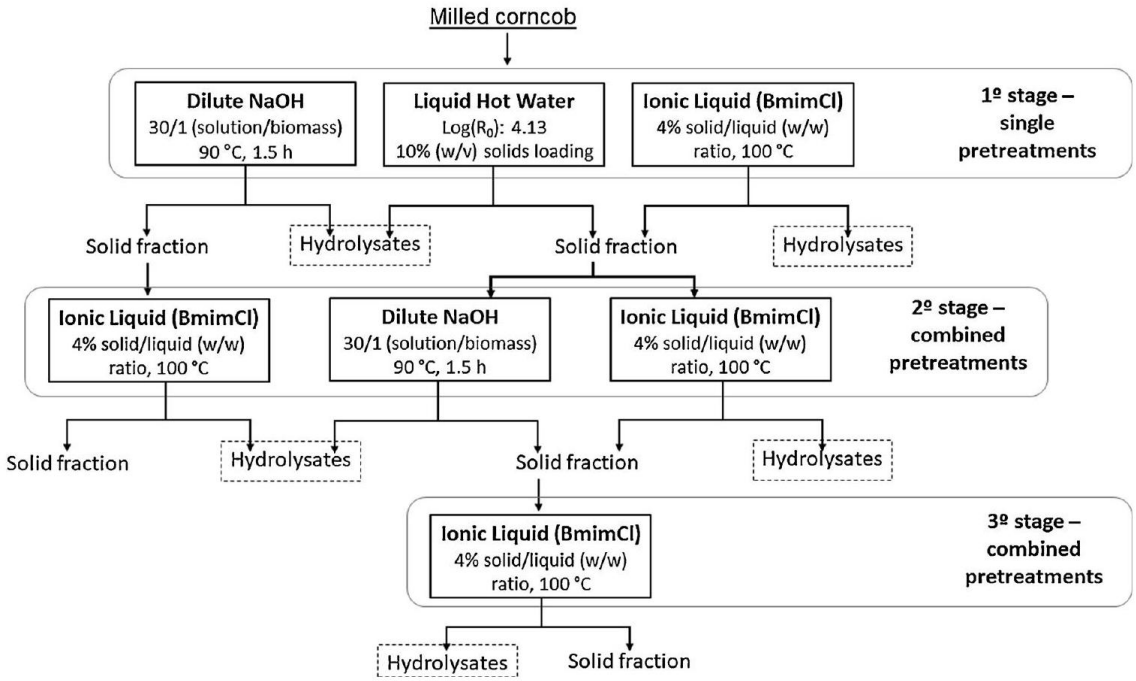

Fig. 1. Schematic representation of pretreatments performed.

Dynamic mechanical analysis

Dynamic mechanical analysis was performed on a PerkinElmer DMA 800 using a dual-cantilever bending mode in order to obtain the storage modulus (E'), the loss modulus (E") and the damping capacity ($\tan \delta$), the latter calculated as the ratio of the loss to the storage modulus. Regenerated films with 20/4/0.015 mm of dimensions, approximately, were analyzed under temperature ranging from 40 to 250°C, heating rate of 5°C/min,

preload 1 N, 10μ m of displacement amplitude and 1 Hz of frequency. Dynamic Young's modulus (E*) was also determined by using Eq. (3) (Menard, 1999).

$$E^* = \sqrt{(E')^2 + (E'')^2} \quad (3)$$

Results and discussion

Compositional analysis

The chemical composition of untreated and treated corncob is presented in Table 1, and images of all samples are presented in Fig. 2. Depending on the treatment type, considerable physical changes, namely color and texture, are noticeable. These changes are mainly due to the removal or not of color-conferring constituents (such as lignin), chemical transformations or changes in crystalline structure.

Table 1
Chemical composition of untreated and pretreated corncob.

Sample	Content (%)			Mass recovery (%)
	Cellulose	Hemicellulose	Lignin	
Corncob	36.35	47.32	16.32	-
IL-CC	39.28	43.70	17.02	90
LHW-CC	78.34	3.95	17.70	59.5
NaOH − CC	64.12	27.88	8.0	46
LHW-IL-CC	80.96	4.02	15.01	56.52
NaOH − IL − CC	67.19	25	7.81	43.2
LHW-NaOH-CC	84.73	4.58	10.68	37.68
LHW-NaOH-IL-CC	86.10	3.53	10.35	36.7

The corncob showed a content of cellulose, hemicellulose and lignin similar to previous studies (Lee et al., 2014; Silvério et al., 2013). It is important to remark that corncob presents also other constituents, such as ash (generally present in percentages around 2.88% $\pm$ 0.11) and extractives (generally present in percentages around 2.1%) (Nabarlatz et al., 2004; Pointner et al., 2014; Silva et al., 2015), which are not accounted in Table 1 because the compositional analysis method applied does not have enough sensitivity to estimate them.

The dissolution (and subsequent regeneration) of corncob in IL did not change significantly its final composition. As it can be seen, the treatment with ionic liquid was only able to remove a small fraction of hemicellulose. However, the physical appearance of the corncob after this treatment changed and seemed to be smoothed, probably due to a structural transformation of cellulose. As expected, the treatment with LHW effectively

solubilized hemicellulose (around 90% of the original content), leading to a final product rich in cellulose and lignin. Other authors have also reported 80-100% of hemicellulose hydrolysis after LHW treatment of lignocellulosic biomass (Liu et al., 2016; Michelin and Teixeira, 2016; Mtui, 2009; Sabanci and Buyukkileci, 2018; Yu et al., 2013). This result also indicates that LHW treatment is not effective in lignin removal, which is in agreement with other published works (Li et al., 2017; Michelin and Teixeira, 2016). It's worth mentioning that, under the treatment conditions chosen, the severity (severity factor, $\log R_0$) of the reaction ($\log R_0 = 4.13$) results in high levels of hemicellulose solubilization, as well as low cellulose depolymerization (Imman et al., 2013; Michelin and Teixeira, 2016; Sabanci and Buyukkileci, 2018). Under this treatment condition, the generation of hydronium ions by ionization of water is known to increase, leading to an effective dissolution of primary products related to hemicellulose constitution (e.g. xylan and acetyl groups) and their subsequent decomposition into oligomers and organic acids, such as acetic acid. This latter auto-catalyze the polysaccharides breakdown into soluble fractions and results in higher hydrolysis efficiency (Imman et al., 2013; Michelin and Teixeira, 2016). As a result of the LHW treatment, substantial morphological changes have been taken on biomass (as will be also shown in Section 3.4 Scanning electron microscopy), which are usually associated with an increase in available surface area and porosity (Imman et al., 2018, 2013; Li et al., 2017). In contrast, the alkali

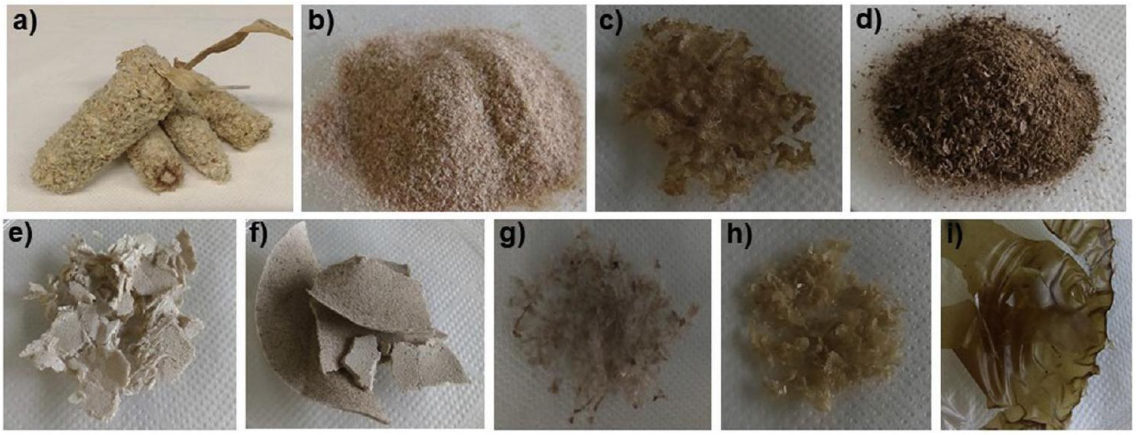

Fig. 2. Photographs of (a) corncob, (b) ground corncob, (c) ionic liquid treated corncob, (d) LHW treated corncob, (e) NaOH treated corncob, (f) LHW-NaOH treated corncob, (g) LHW-NaOH-IL treated corncob, (h) NaOH-IL treated corncob and (i) LHW-IL treated corncob.

treatment removed mainly the lignin fraction. A lignin content reduction by 50% resulted in a mass loss at around half of the original weight of the untreated corncob on a dry basis. Moreover, by removing lignin, the alkali treatment partially disrupts the linkages between the lignin and hemicellulose, and consequently solubilizes hemicellulose (its reduction can be noticed in Table 1).

Regarding the combined pretreatments, even after the prior changes and weakening of corncob structure reached through the LHW treatment, the subsequent dissolution in BmimCl only removed a small amount of the remaining lignin. Conversely, the regenerated product presents a smooth and homogenized morphology, as well as a film-like aspect (Fig. 2), which proves that, by removing hemicellulose, the LHW treatment increased the accessibility of cellulose and favored its dissolution in BmimCl. Minor effects on chemical composition have also been noticed by combining NaOH and IL treatments

(Table 1). In line with other studies, these results demonstrate the low capacity of the BmimCl in fractionating the biomass (Geng and Henderson, 2012; Mahmood et al., 2016). On the opposite, remarkable changes were verified by combining LHW with alkali treatment. This can be explained by the solubilization of most hemicellulose during the LHW treatment, the disruption of the lignin-hemicellulose complexes and a decrease in β-O-4 linkages of lignin (the most abundant substructure in this component) also took place, which makes the lignin more accessible (Imman et al., 2018; Li et al., 2017). Consequently, the cleavage of ester, ether and carbon-to-carbon bonds between lignin-cellulose, lignin components (e.g. syringyl and guaiacyl monolignols) and the remaining lignin-hemicellulose complexes was easier during the alkaline treatment, leading to the breaking of lignin into small molecules and their dissolution. The broken of lignin structure and its decoupling with carbohydrates are confirmed and easily identified by FTIR analysis (Fig. 3). Their complementary and selective effects of LHW and NaOH treatments on fractionating the biomass contributed positively to obtain a solid cellulose-enriched final product (84.73%), with reasonably low amounts of hemicellulose (reduced by 90%) and lignin (reduced by 34.5%). This result is comparable to the ones archived by established laboratory methods for delignification in which, besides alkaline, acidic and oxidative reagents are used. Little improvements have been made to the fractionation process by combining LHW, NaOH and IL treatments. However, the dried regenerated material was semitransparent and had a plastic film-like appearance (Fig. 2g), completely different from the starting material (Fig. 2f). This physical characteristic suggests a decrease in the Crl of the sample in response to an amorphous conversion, as it will be, indeed, confirmed and explored in detail in the following analysis.

Fourier-transformed infrared spectroscopy

FTIR spectra of untreated and treated corncob are shown in Fig. 3. The broad band observed at $3000 - 3700\ cm^{-1}$ is assigned to different OH stretching of cellulose and hemicellulose (Ma et al., 2015; Rhim et al., 2015). The peak absorption at $1640\ cm^{-1}$, typical of absorbed water in biomass, was also verified in all samples analyzed (Poletto et al., 2013). From Fig. 3, well defined common bands typical of functional groups in cellulose were identified at $3000 - 3700\ cm^{-1}(O - H$ stretching), $2919\ cm^{-1}$ (C-H stretching vibration), $1420\ cm^{-1}(CH_2$ banding vibration), $1374\ cm^{-1}$ (C-H asymmetric deformation), $1318\ cm^{-1}$ (CH_2 wagging), $1164\ cm^{-1}$ (asymmetric C-O-C stretching), $1114\ cm^{-1}$ (C-OH skeletal vibration), $1059\ cm^{-1}$ (C-O-C pyranose ring skeletal vibration) and $897\ cm^{-1}$ (C-H deformation vibration, characteristic of the β-glycosidic linkages between glucose monomers) (Ang et al., 2012; Ma et al., 2015; Poletto et al., 2013; Reddy et al., 2017; Wang et al., 2017). As it can be seen in Fig. 3a and b, all typical bands of cellulose can be easily identified in the spectrum after NaOH and LHW-NaOH treatments. Besides, notable bands at around 1730 (acetyl group in hemicellulose), $1250\ cm - 1$ (C-O stretching in the arylether group of lignin and acetyl groups in hemicellulose), 1598 and 1513 (in response to aromatic ring stretch ascribed to lignin), are notice mainly in the raw corncob spectrum (Fig. 3a), which were attributed to the presence of hemicellulose and lignin (Ma et al., 2015; Reddy et al., 2017). The intensity of these bands has become significantly reduced after LHW-NaOH and NaOH treated corncob, which evidences their better capacity to partially fractionate and remove non-cellulosic components of corncob.

Less noticeable chemical changes were observed on the spectra after other treatments, such as LHW and IL (Fig. 3a), mainly due to the high content of lignin remaining in the biomass after treated. However, the appearance of peaks at 1420 and $1114\ cm - 1$ (in the LHW treated sample) and the more pronounced peak at $1059\ cm^{-1}$ in both treatments,

compared to those in raw corncob, suggest a higher cellulose content. Table 2 shows the main absorption bands and the respective group of cellulose, as well as treated and untreated biomass samples.

FTIR spectra can also be applied to investigate changes in cellulose crystalline structure. In the cell wall of plants, cellulose mainly contains cellulose crystalline I, but, depending on the type of processing and treatment to which it is submitted, this primary structure can be transformed into other allomorphic forms, such as amorphous cellulose and cellulose crystalline II (Cheng et al., 2012; Heinze, 2016; Reddy et al., 2017; Zhang et al., 2014). Variations in the absorption bands around 1425, 1370, 1157, 1108 and 898 cm^{-1}, typical of cellulose I, can be used as an indication of crystalline structural transformations (Poletto et al., 2013; Reddy et al., 2017; Rhim et al., 2015). From the

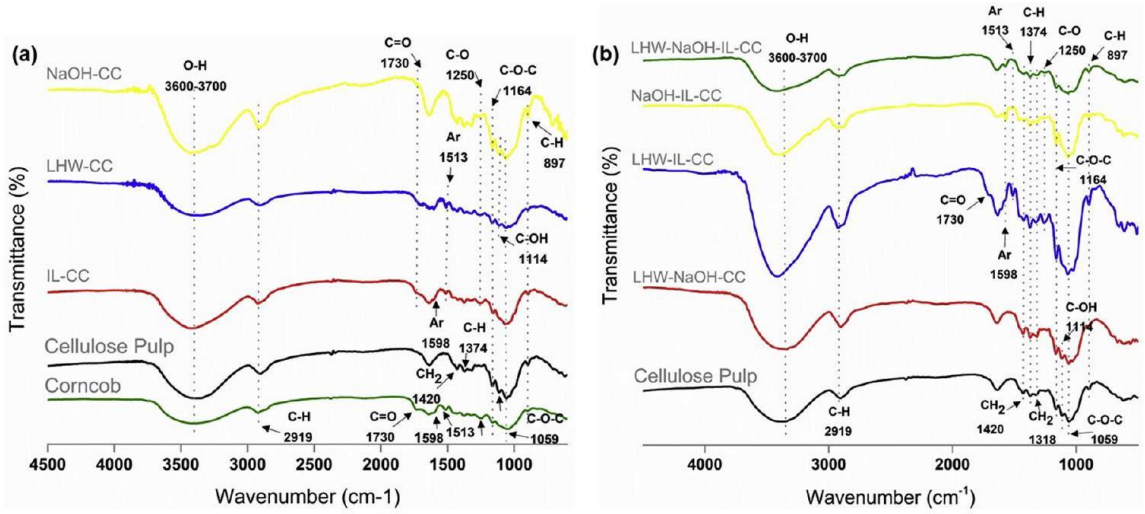

Fig. 3. FTIR spectra of (a) cellulose pulp, corncob and single pretreatments and cellulose pulp spectrum in Fig. 3, it is possible to assume that characteristic bands at 1420,1114 and 897 cm^{-1} correspond to cellulose crystalline I. Among the treatments performed, those involving the dissolution of cellulosic biomass with ionic liquid significantly decreased the intensity of bands at 1420 and 1114 cm^{-1}, while the absorption intensity band at 897 cm^{-1} increased after LHW-IL treatment and kept unchanged after NaOH -IL and LHW-NaOH-IL treatments. Moreover, from ionic liquid combined treatments spectrum, it is visible that the peaks assigned to $O-H$ stretching vibrations ($3000-3700\ cm^{-1}$) became sharper, probably due to the scission of intra- and intermolecular hydrogen bonds (Ciolacu et al., 2011). The FTIR spectra of BmimCl treated samples seems to be typical of amorphous cellulose, although they also resemble cellulose crystalline II (Ciolacu et al., 2011; Reddy et al., 2017). These crystalline structural changes will be clearly elucidated with the XRD analysis, which will confirm that the combined IL treatments result mainly in amorphous cellulose.

X-ray diffraction analysis

X-ray diffractograms of cellulose pulp, corncob and all treated samples are shown in Fig. 4. Diffractograms of cellulose pulp and samples treated with LHW, NaOH and $LHW-NaOH$ present three major peaks, typical of cellulose crystalline I. The main peak position varies with sample analyzed from $2\theta = 22.2°$ to $2\theta = 22.6°$. This peak is indicative of the distance

between hydrogen-bonded sheets in cellulose crystalline I. The second peak, viewed as a wide peak at lower 2θ values, is known to be correlated to allomorphs of cellulose crystalline I, (b) combined pretreatments. Abbreviation Ar in graphs means aromatic ring. and varies from 15.5° to 16°. The third is depicted as a small peak at 34.7° and arises from ordering along the fiber direction (Ahvenainen et al., 2016; Cheng et al., 2011; Ciolacu et al., 2011; Park et al., 2010; Thygesen et al., 2005). The CrI of samples was determined by the Segal method (Segal et al., 1959) as specified in Section 2.5.4 of the materials and methods. This method provides a faster and useful measurement for comparing the relative differences of CrI among samples. In the literature several different techniques are reported to measure CrI, and depending on the chosen method the CrI can vary significantly (Park et al., 2010). The obtained CrI values of cellulose pulp ($\mathrm{CrI} = 70$), corncob ($\mathrm{CrI} = 30$) and samples treated with $\mathrm{LHW}(\mathrm{CrI} = 50)$, NaOH ($\mathrm{CrI} = 63$) and $\mathrm{LHW} - \mathrm{NaOH}(\mathrm{CrI} = 67)$ are shown in Fig. 4a and b. The high CrI of samples treated with LHW, NaOH and LHW-NaOH, in comparison to the corncob, can be related to the removal of non-cellulosic components. Despite the high cellulose content in LHW-CC sample, it still presents a reasonable percentage of lignin (Table 1), which is closely associated with cellulose microfibrils and directly affects the crystallinity. It can also be observed that LHW-NaOH treated sample presented CrI value very close to the cellulose pulp, and from the high-intensity peak at 34.7° is possible to deduce that this sample has a greater ordering of fibers.

Samples subjected to combined treatments with ionic liquid (Fig. 4b) gave diffractograms that clearly support the previous results obtained by FTIR. In general, a strong reduction of peaks around $2\theta = 22°$ and 23° and $2\theta = 15°$ is observed, as well as the appearance of a single broad peak extending from 15° to 22.5°, which are characteristic of amorphous cellulose (Ciolacu et al., 2011; Park et al., 2010). In

Table 2
FTIR absorbance bands and the respective functional groups in cellulose pulp, untreated and treated corncob.

Wavenumber (cm^{-1})	Chemical group	assignment	Reference
3000-3700	O-H	O-H stretching of cellulose and hemicellulose	(Ma et al., 2015; Rhim et al., 2015)
2919	C-H	C-H stretching in cellulose-rich material	(Ang et al., 2012)
1730	$\mathrm{C} = \mathrm{O}$	$\mathrm{C} = \mathrm{O}$ stretching of acetyl group in Hemicellulose and aldehyde in lignin	(Ma et al., 2015; Reddy et al., 2017)
1640	O-H	O-H bending vibration of absorbed water molecules	(Reddy et al., 2017; Wulandari et al., 2016)

1598 and 1513		Aromatic ring (Ar) stretch ascribed to lignin	(Ang et al., 2012; Kristensen et al., 2008)
1420	CH_2	CH_2 banding vibration in cellulose	(Reddy et al., 2017)
1374	$C-H$	$C-H$ asymmetric deformation in cellulose	(Reddy et al., 2017)
1318	CH_2	CH_2 Wagging in cellulose	(Reddy et al., 2017)
1250	$C-O$	C-O stretching in the aryl group of lignin and acetyl groups of hemicellulose	(Yu et al., 2014)
1164	C-O-C	Asymmetric C-O-C stretching ascribed to cellulose	(Poletto et al., 2013; Wang et al., 2017)
1114	C-OH	$C-OH$ skeletal vibration in cellulose	(Wang et al., 2017)
1059	C-O-C	C-O-C pyranose ring skeletal vibration ascribed to cellulose	(Wang et al., 2017; Wulandari et al., 2016)
897	C-H	C-H deformation of cellulose	(Ang et al., 2012; Poletto et al., 2013; Wang et al., 2017)

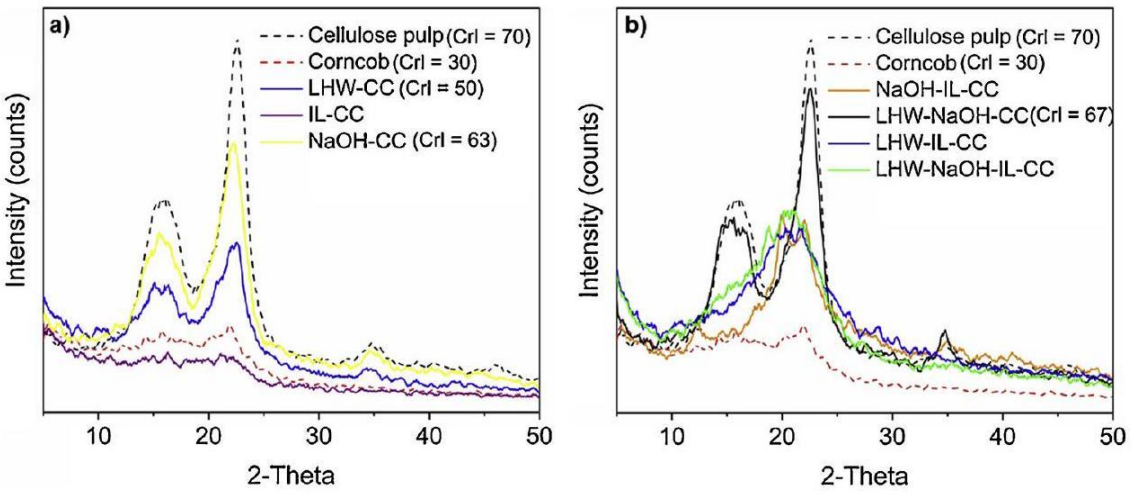

Fig. 4. X-ray diffractograms of (a) cellulose pulp, corncob and single pretreatments and (b) combined pretreatments.

fact, throughout the dissolution of cellulosic biomass in BmimCl, initially the cations and anions of the IL come into contact with the hydrogen bonds $C2-O$ and $C6-O$ of cellulose, forming new H -bonds and making the surface chains swelling, followed by the gradually peeled of its chains and the breaking of C3-O hydrogen bonds, which result in the partial or complete dissolution of cellulose (Li et al., 2018). As a result of the hydrogen bond network disruption, the cellulose is not allowed to recrystallize during the fast regeneration process and settles as an amorphous form (Cheng et al., 2011; Dadi et al., 2006; Gupta and Jiang, 2015). Similar results were reported by Geng and Henderson (2012); Singh et al. (2013) and Reddy et al. (2017). Amorphous structures were also obtained by Dadi et al. (2006) independent time dissolution in BmimCl and the regeneration medium.

Especially for the NaOH -IL-CC regenerated sample, three distinct diffracted peaks appeared at $2\theta = 12.2°, 19.9°$ and $22°$ (Fig. 4b). The emerging of these peaks, along with the spectra shape, might suggest a possible conversion from cellulose crystalline I to II (Ciolacu and Valentin, 2006; Reddy et al., 2017), but actually these features result from the conversion of cellulose crystalline I to amorphous cellulose and the high amount of hemicellulose embedded in this sample. As a consequence of this amorphous conversion after IL treatment, the crystalline peaks identified in the NaOH pretreated samples were reduced and the diffracted peaks related to hemicellulose, typically located around $2\theta = 12.4°$ and $2\theta = 19.1°$ (Zhang et al., 2016), were emphasized, given rise to the concerned diffractogram shown in Fig. 4b. In addition, the high content of hemicellulose in this sample seems to have a negative effect on cellulose dissolution, since the peak at $2\theta = 34.7°$ associated with the cellulose crystalline I can be notice in the NaOH -IL-CC spectra. Therefore, it is possible to assume that, besides the high hemicellulose content, the NaOH -IL combined treatment results in a cellulosic biomass sample composed mainly by amorphous cellulose and lesser amounts of cellulose crystalline I. This result is also supported by the low temperature of maximum rate of weight loss related to this sample (Fig. 6b) verified through thermogravimetric analysis.

Regarding the raw corncob, there were no significant changes between the patterns of untreated and only IL-treated, except for a decrease in the intensity of curve related to the IL-CC (Fig. 4a). Therefore, from the obtained results it is possible verifying that,

independent of the pretreatment applied prior to dissolution in BmimCl, amorphous cellulose is the dominant structure in the regenerated samples.

Scanning electron microscopy

SEM study of samples (Fig. 5) shows that untreated corncob has a rigid, porous and irregular morphology assembled into compact layers with different surface textures. Corncob is made up of different components, namely the beeswing, coarse chaff and woody ring, which confers stiffness, and the pith, the innermost part of the cob, with a consistency similar to foam plastic (Matsushima et al., 1957). Each component has different morphology, constitution (regarding the content of cellulose, hemicellulose, lignin and waxes), and consequently different physicochemical features, which may play an important role in the characteristics of the material obtained after the pretreatments. From Fig. 5e it is clear that the morphology of BmimCl treated corncob remained relatively unchanged (no defibrillation process can be seen), only smoothing and homogenization of the surface were observed. After the treatment with LHW considerable morphological changes became evident. The defibrillation process, resulting mainly from the removal of hemicellulose, partly collapsed the cell wall of corncob, leading to an increase in available surface area and porosity. Imman et al. (2018) showed that, under the same severity factor, the LHW treatment could duplicate the available surface area of corncob. However, due to the large amount of residual lignin remaining in biomass, the cellulose fibers have kept still arranged together in large bundles. Contrarily, the treatment with NaOH could dissolve bulk and inter-fibrillar lignin, leading to the disruption and disaggregation of biomass fibers.

As a result of the combined LHW-NaOH treatment, more uniform fiber distribution and a remarkable disaggregation are noticed (Fig. 5d). By promoting the initial defibrillation of the biomass, the previous treatment conducted with LHW increased the accessibility to the complex lignin-cellulose matrix and enhanced the performance of the alkaline treatment. In general, cellulosic fibers with different shapes, sizes and rough surface topography were obtained at the end of the treatment (probably due to the mix of components that make up the corncob). Except for the average diameter of the longer fibers, the characteristics of LHW-NaOH-CC extracted fibers hardly resemble the cellulose pulp fibers (Fig. 5d and i). This can be simply explained by the different morphology inherent to the corresponding plant sources and the effect of different background processing/treatments applied to both samples.

Regarding the combined treatments with BmimCl (Fig. 5f, *g* and h), the obtained regenerated material had no fibrous aspect and a smooth and uniform surface. Similar regenerated products were also observed by Geng and Henderson (2012), Abdulkhani et al. (2013) and Reddy et al. (2017), who performed the dissolution of other cellulosic biomass with ionic liquids and obtained regenerated materials with a flat surface.

Thermogravimetric properties

The thermal properties of all samples were investigated by TG and DSC, as illustrated in Fig. 6. The temperature at which the degradation processes start (T_{onset}, °C), the temperature of maximum rate of weight loss (T_{max}, °C), the weight loss (%) /WL) and the enthalpy of melting (ΔH_f, J/g) for all samples are presented in Table 3. Herein, T_{onset} will

be

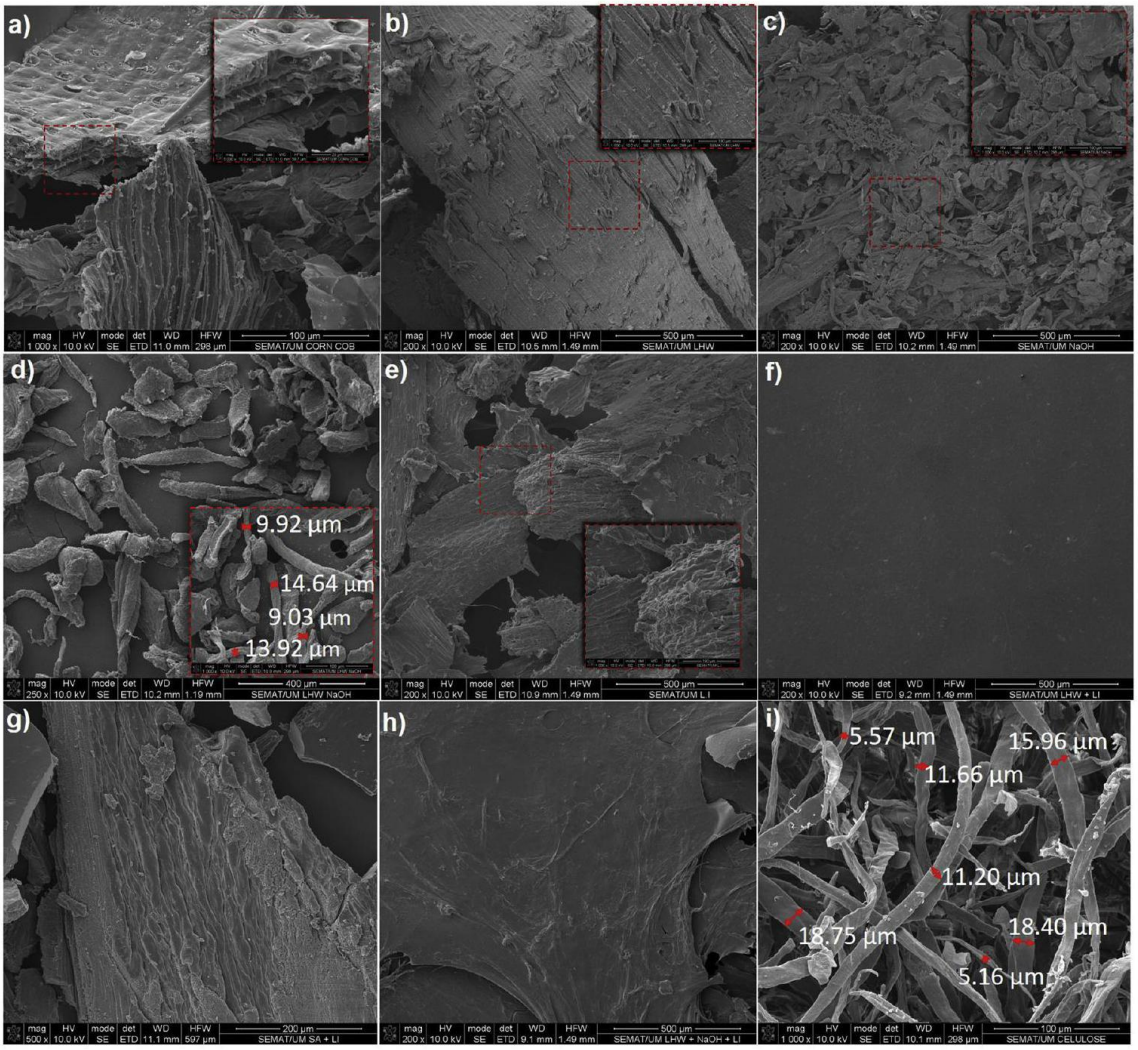

Fig. 5. SEM micrographs of (a) untreated corncob, (b) LHW-CC, (c) NaOH-CC, (d) LHW-NaOH-CC, (e) IL-CC, (f) LHW-IL-CC, (g) NaOH-IL-CC, (h) LHW-NaOH-IL-CC and (i) Cellulose Pulp.

considered as the temperature at which the process of decomposition starts, excluding the initial mass loss that was due to water evaporation. When it turns to lignocellulosic biomass, T_{onset} corresponds to the temperature at which low molar mass substances start to degrade, such as hemicellulose and possibly some lignin. Along with the T_{max}, T_{onset} will be used to evaluate the thermal stability conferred to the lignocellulosic fibers of corncob after pretreatments. Besides, data regarding the thermal process in Table 3 are discretized into two phases, that arise, in some samples, as an effect of the chemical composition or physicochemical changes after the pretreatments.

From the thermograms exhibited in Fig. 6, it is noticeable that the pretreatments performed had a remarkable effect over the thermal decomposition process. A small weight loss at lower temperatures (< 150°C) due to water evaporation or low molecular

weight

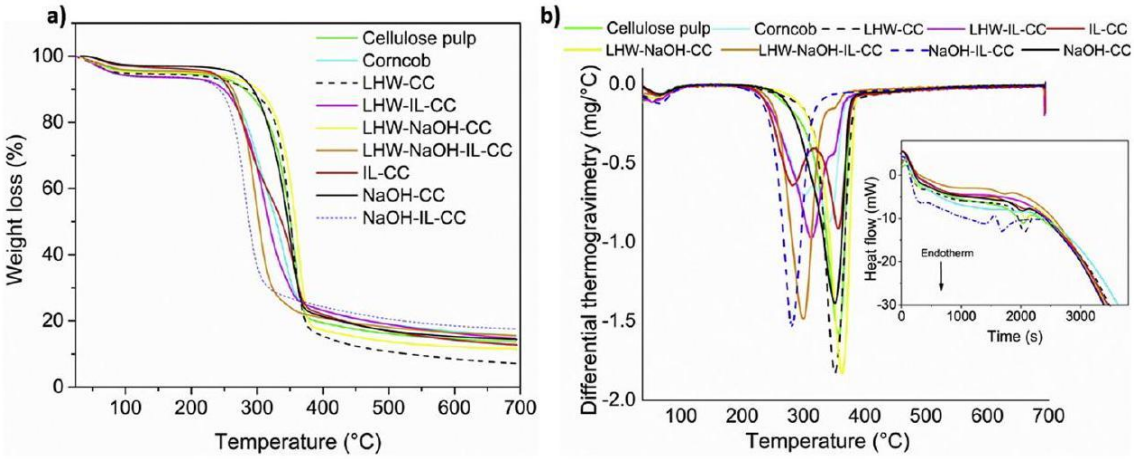

Fig. 6. (a) TGA, (b) DTG and DSC (inset plot in the graph 5b) curves of the cellulose pulp, untreated and treated corncob.

Table 3
Thermogravimetric results for cellulose pulp, untreated and treated corncob samples.

Sample	T_{onset} (°C)	Phase I		Phase II		Enthalpy (J/g)
		Tmax (°C)	WL (%)	Tmax (°C)	WL (%)	
Cellulose pulp	275	357	72.8			101.6
Corncob	240	301	38	342	30.65	2.5
IL	247	282	37.5	356	34	2.1
LHW	294	351	75.17			233.3
NaOH	275	351	72.2			43
LHW + IL	241	313	60.6	348	8.6	n.d.
LHW + NaOH	294	363	75.45			104.5
LHW + NaOH + IL	252	300	70.47	348	2.9	56.6
NaOH + IL	238	277	64.7			38.8

compounds is observed in all curves. Two other distinct peaks characteristic of hemicellulose and cellulose decomposition are observed at temperatures between 200 and 400°C. Due to the wide temperature degradation range of lignin (200 – 600°C), it overlaps

partially with cellulose and hemicellulose thermal decomposition curves and, consequently, does not present maximum weight loss rate (Yue et al., 2015; Zhang et al., 2014). In general, with exception of combined treatments with ionic liquid, all the pretreatments increased the thermal stability of fibers compared to the corncob raw fibers.

The thermal profiles related to LHW-CC and NaOH-CC pretreated samples present single step with a narrow temperature range. In comparison to the cellulose pulp curve, the LHW-CC profile has a slightly lower T_{max} derived mainly from its rather high content of lignin. However, its T_{onset} increased significantly in comparison to the corncob profile as a result of the effective hemicellulose solubilization during the LHW treatment. Similar T_{max} value is also displayed by the NaOH treated sample, but due to the high content of hemicellulose embedded in this sample, it presents a broad curve base.

Degradation reactions observed in the curve associated to LHWNaOH pretreated sample occurred in a single step and in a narrow temperature range, similar to the cellulose pulp curve, which decomposes in a narrow range between 275 and 400°C (Fig. 6a). The results evidence that this pretreatment had the best performance in terms of hemicellulose and lignin removal, resulting in a product composed mainly of cellulose, as evidenced by the other analysis performed. Compared to the single pretreatments, the combination between LHW and dilute NaOH solution resulted in a narrower and stable degradation curve, with higher T_{max}. By removing the amorphous hemicellulose and the aromatic rings of lignin, the thermal stability of fibers was increased in response to the high crystallinity of the remaining cellulose chains. The final product obtained after the coupled treatment of LWH-NaOH (T_{onset} of 294°C and T_{max} of 363°C) presented higher thermal stability than the cellulose pulp (T_{onset} of 275°C and T_{max} of 357°C), which might be probably related to the different biological sources of cellulose.

In contrast, despite the increased thermal stability of the crude substrate after ionic liquid treatment, this study suggests that the BmimCl presents reduced performance on the fractionation of lignocellulosic biomass, which is in agreement with other studies (Mahmood et al., 2016; Gräsvik et al., 2014; Swatloski et al., 2002 and Geng and Henderson, 2012). As shown in Fig. 6, the IL-CC degradation profile can be discretized into two phases and presents two weight loss regions between 200 and 400°C (Fig. 6 and Table 3). The first peak, with corresponding T_{max} of 282°C, is related to hemicellulose degradation, while the second assigns to the cellulose degradation, with corresponding T_{max} of 356°C. Few changes are verified when compared to the raw corncob profile. Moreover, when applied in combination with other treatments, the ionic liquid decreased the thermal stability of fibers and displaced T_{max} to lower values. Such effects can be attributed to the conversion of the native cellulose (cellulose crystalline I) to an amorphous structure, which is in agreement with the results obtained in the other analysis. The IL treatment gave rise to a second phase identified by a shoulder-like around 350°C in the differential thermogravimetry profiles. This temperature is typical of cellulose decomposition and thus confirms the coexistence of cellulose crystalline I. The application of previous treatments on corncob decreased its recalcitrant property and provided the direct interaction of the ionic liquid with the cellulose, which, in turn, causes the rupture of more intermolecular and intramolecular hydrogen bonds of original cellulose during the dissolution process. The same was not observed in the direct treatment of the corncob with ionic liquid, since the cellulose dissolution was hindered by the dense packaging of hemicellulose and lignin and the high viscosity of the ionic liquid, limiting its performance to components more easily hydrolyzable. Particularly for the NaOH-IL sample, the lowest T_{max} value verified is

greatly attributed to the high amount of hemicellulose remained after the treatments, which presents maximum rate of weight loss around 300°C.

From DSC results in Fig. 6 (inset plot in graph 6b), all samples presented endothermic peaks consistent with T_{max} from DTG, which are attributed to the depolymerization of cellulosic and non-cellulosic components. DSC results indicated that the melting enthalpy of the treated samples with IL was drastically reduced compared to the native cellulose and other treatments (Table 3), which can be associated to both a decrease of hydrogen bonds and crystallinity of cellulose (Filho et al., 2000; Wan Daud and Djuned, 2015). Thus, all the results demonstrate that the treatment with IL converted the native cellulose mostly to an amorphous and less thermally stable structure, which corroborates with XRD analysis.

Dynamic mechanical analysis and chemical characterization of regenerated film

Through dissolution with IL and regeneration in deionized water, attempts to produce regenerated films from the previously pretreated samples were made. However, the only sample suitable to produce films resulted from the LHW-NaOH combined treatment. Due to the remaining reasonably amounts of lignin and hemicellulose in other samples the obtained films were very brittle films and impossible to be analyzed via DMA. The suitability of samples to produce regenerated films supports the previous chemical characterization discussions, from which the superior fractionation capacity of the LHW-NaOH combined treatment was revealed.

Briefly, the regenerated cellulose film presents a uniform and dense smooth surface (Fig. 7c and d), as well as chemical characteristics similar to that of LHW-NaOH-IL pretreated sample (regenerated as a gel), as can be seen by comparing Figs. 3, 4 and 7b. Both samples also presented similar thermal properties (not shown). Therefore, it is clear that the different regeneration techniques and anti-solvents applied did not change the chemical structure or influence the formation of crystalline phases, but only resulted in different regenerated shapes. Thus, the regenerated film prepared from the LHW-NaOH-IL combined treatment sample is not included in the following discussions.

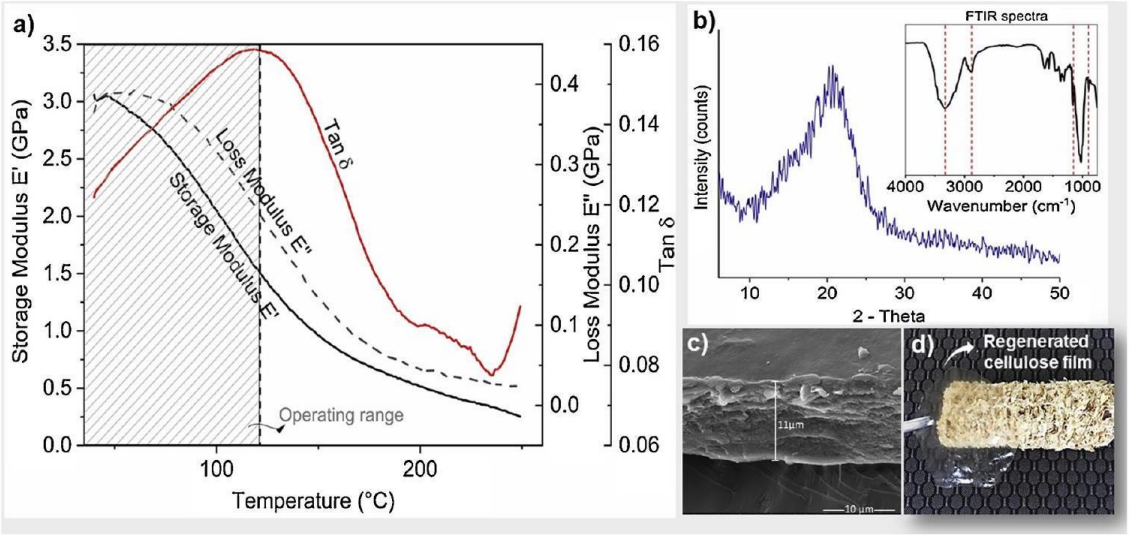

Fig. 7. (a) Dynamic mechanical analysis, (b) X-ray diffraction and FTIR spectra (inset graph in Fig. 7b) and (c) SEM cross section of (d) regenerated cellulose film produced from LHW-NaOH pretreated corncob.

Fig. 7a shows the viscoelastic properties of the produced regenerated film, E' and E" drop as the temperature increases. The transparency of the film (Fig. 7d) is also indicative of its amorphous state, since this property is related to the unpackaging of cellulose chains. The operating range of the regenerated film was limited by the glass transition temperature (T_g), which was found as 120°C, approximately, and determined through the peak of tan δ curve. Similar T_g values of other regenerated cellulose films were reported by Yeng et al. (2015) and Ioelovich (2016). From this temperature, the physical properties of the film may change greatly, which end up compromising its performance depending on the intended application. Moreover, from approximately 75°C the loss modulus drops markedly, and the mechanical deformation applied begins to be converted into internal friction and nonelastic deformation.

As a new material for potential applications it is important to determine the storage modulus and the dynamic Young's modulus, as they quantity the material's stiffness. Taking as reference the values at 40°C, E' and E* are 3.04 GPa and 3.06 GPa , respectively. These values are higher than regenerated films produced from cotton linter pulp -2.54 – 5GPa (Ashok et al., 2015; Qi et al., 2009), Polylactic acid (PLA) 2 GPa (Kamthai and Magaraphan, 2015), PLA/bamboo fabric laminate - 1.75 GPa (Porras and Maranon, 2012), microcrystalline cellulose 2.57 GPa (Duchemin et al., 2009) and bleached hardwood kraft pulp 1.5 GPa (Zhang et al., 2018). The results presented suggest that the regenerated cellulose, produced herein via a sustainable processing from corncob residues, could be potentially used in value-added applications, such as packaging.

Conclusions

In this study, corncob was pretreated by performing individual and combined green pretreatments, namely liquid hot water and ionic liquid (BmimCl), as well as dilute NaOH solution, and attempts to produce regenerated cellulose films were carried out through dissolution of pretreated samples in BmimCl. The results confirmed the low fractionation

capacity of BmimCl and the complementary effects of LHW (which efficiently removed hemicellulose) and NaOH (efficient in lignin removal). The disruption of hemicellulose and the subsequent weakening of the biomass structure resulting from the LHW treatment increased the accessibility of lignin. Therefore, the combined LHW-NaOH pretreatment was very efficient at removing the non-cellulosic components from corncob and leads to a solid enrich-cellulose fraction with high crystallinity and thermal stability. The results also revealed that, regardless of the pretreatment applied prior to dissolution in BmimCl, the regenerated samples were constituted mainly by amorphous structure.

This work shows the efficient application of some combined green and conventional treatments, with results comparable with those obtained by established laboratory methods for delignification. The results also revealed that, suitability of biomass to different types of valorization can be optimized by pretreatments combination. Moreover, the high stable and crystalline cellulose obtained after LHW-NaOH combine treatment gave rise to a regenerated film with outstanding viscoelastic properties, suitable for packaging applications. The sequential process design involving combined green pretreatments and ionic liquid dissolution to produce regenerated cellulose films can be seen as a sustainable approach, but it is still challenging in terms of costs and scalability. Nevertheless, the development of life cycle and costs assessment can give more insights on the feasibility, design and optimization of this production method.

References

Abdulkhani, A., Hojati Marvast, E., Ashori, A., Karimi, A.N., 2013. Effects of dissolution of some lignocellulosic materials with ionic liquids as green solvents on mechanical and physical properties of composite films. Carbohydr. Polym. 95, 57-63. https://doi.org/10.1016/j.carbpol.2013.02.040.

Agbor, V.B., Cicek, N., Sparling, R., Berlin, A., Levin, D.B., 2011. Biomass pretreatment: fundamentals toward application. Biotechnol. Adv. 29, 675-685. https://doi.org/10.1016/j.biotechadv.2011.05.005.

Ahvenainen, P., Kontro, I., Svedström, K., 2016. Comparison of sample crystallinity determination methods by X-ray diffraction for challenging cellulose I materials. Cellulose 23, 1073-1086. https://doi.org/10.1007/s10570-016-0881-6.

Ang, T.N., Ngoh, G.C., Seak, A., Chua, M., Lee, M.G., 2012. Elucidation of the effect of ionic liquid pretreatment on rice husk via structural analyses. Biotechnol. Biofuels 5, 1-10.

Araújo, D.J.C., Machado, A.V., Vilarinho, M.C.L.G., 2018. Availability and suitability of agroindustrial residues as feedstock for cellulose-based materials: Brazil case study. Waste Biomass Valorization 16. https://doi.org/10.1007/s12649-018-0291-0.

Ashok, B., Reddy, K.O., Madhukar, K., Cai, J., Zhang, L., Rajulu, A.V., 2015. Properties of cellulose/Thespesia lampas short fibers bio-composite films. Carbohydr. Polym. 127, 110-115. https://doi.org/10.1016/j.carbpol.2015.03.054.

Bhutto, A.W., Qureshi, K., Harijan, K., Abro, R., Abbas, T., Bazmi, A.A., Karim, S., Yu, G., 2017. Insight into progress in pre-treatment of lignocellulosic biomass. Energy 122, 724-745. https://doi.org/10.1016/j.energy.2017.01.005.

Brandt, A., Gräsvik, J., Hallett, J.P., Welton, T., 2013. Deconstruction of lignocellulosic biomass with ionic liquids. Green Chem. 15, 550-583. https://doi.org/10.1039/c2gc36364j.

Brodin, M., Vallejos, M., Tanase, M., Cristina, M., Chinga-carrasco, G., 2017. Lignocellulosics as sustainable resources for production of bioplastics e A review. J. Clean. Prod. 162, 646-664. https://doi.org/10.1016/j.jclepro.2017.05.209.

Capolupo, L., Faraco, V., 2016. Green methods of lignocellulose pretreatment for biorefinery development. Appl. Microbiol. Biotechnol. 100, 9451-9467. https://doi.org/10.1007/s00253-016-7884-y.

Carrier, M., Loppinet-Serani, A., Denux, D., Lasnier, J.-M., Ham-Pichavant, F., Cansell, F., Aymonier, C., 2011. Thermogravimetric analysis as a new method to determine the lignocellulosic composition of biomass. Biomass Bioenergy 35, 298-307. https://doi.org/10.1016/j. biombioe. 2010.08.067.
Chen, H., Liu, J., Chang, X., Chen, D., Xue, Y., Liu, P., Lin, H., Han, S., 2017. A review on the pretreatment of lignocellulose for high-value chemicals. Fuel Process. Technol. 160, 196-206. https://doi.org/10.1016/j.fuproc.2016.12.007.
Chen, T., Li, L., Zhao, R., Wu, J., 2016. Pyrolysis kinetic analysis of the three pseudocomponents of biomass-cellulose, hemicellulose and lignin: sinusoidally modulated temperature method. J. Therm. Anal. Calorim. 128, 1825-1832. https://doi.org/10. 1007/s10973-016-6040-3.
Chen, Y., Stevens, M.A., Zhu, Y., Holmes, J., Xu, H., 2013. Understanding of alkaline pretreatment parameters for corn stover enzymatic saccharification. Biotechnol. Biofuels 6, 1. https://doi.org/10.1186/1754-6834-6-8.
Cheng, G., Varanasi, P., Arora, R., Stavila, V., Simmons, B.A., 2012. Impact of ionic liquid pretreatment conditions on cellulose crystalline structure using 1 - Ethyl-3-methylimidazolium acetate. J. Phys. Chem. 10049-10054. https://doi.org/10.1021/jp304538v.
Cheng, G., Varanasi, P., Li, C., Liu, H., Melnichenko, Y.B., Simmons, B.A., Kent, M.S., Singh, S., 2011. Transition of cellulose crystalline structure and surface morphology of biomass as a function of ionic liquid pretreatment and its relation to enzymatic hydrolysis. Biomacromolecules 12, 933-941. https://doi.org/10.1021/bm101240z.
Ciolacu, D., Ciolacu, F., Popa, V.I., 2011. Amorphous cellulose - structure and characterization. Cellul. Chem. Technol. 45, 13-21. https://doi.org/10.1163/156856198X00740.
Ciolacu, D., Valentin, I.P., 2006. On the thermal degradation of cellulose allomorphs. Cellul. Chem. Technol. 40, 445-449.
Dadi, A.P., Varanasi, S., Schall, C.A., 2006. Enhancement of cellulose saccharification kinetics using an ionic liquid pretreatment step. Biotechnol. Bioeng. 95, 904-910. https://doi.org/10.1002/bit.
Daza Serna, L.V., Orrego Alzate, C.E., Cardona Alzate, C.A., 2016. Supercritical fluids as a green technology for the pretreatment of lignocellulosic biomass. Bioresour. Technol. 199, 113-120. https://doi.org/10.1016/j.biortech.2015.09.078.
Duchemin, B.J.C., Newman, R.H., Staiger, M.P., 2009. Structure-property relationship of all-cellulose composites. Compos. Sci. Technol. 69, 1225-1230. https://doi.org/10.1016/j.compscitech.2009.02.027.
Farrán, A., Cai, C., Sandoval, M., Xu, Y., Liu, J., Hernáiz, M.J., Linhardt, R.J., 2015. Green solvents in carbohydrate chemistry: from raw materials to fine chemicals. Chem. Rev. 115, 6811-6853. https://doi.org/10.1021/cr500719h.
Filho, G.R., Da Cruz, S.F., Pasquini, D., Cerqueira, D.A., Prado, V.D.S., De Assunção, R.M.N., 2000. Water flux through cellulose triacetate films produced from heterogeneous acetylation of sugar cane bagasse. J. Memb. Sci. 177, 225-231. https://doi.org/10.1016/S0376-7388(00)00469-5.
Fort, D.A., Remsing, R.C., Swatloski, R.P., Moyna, P., Rogers, R.D., 2007. Can ionic liquids dissolve wood? Processing and analysis of lignocellulosic materials with 1 – n -butyl-3-methylimidazolium chloride. R. Soc. Chem. 63-69. https://doi.org/10. 1039/b607614a.
Geng, X., Henderson, W.A., 2012. Pretreatment of corn stover by combining ionic liquid

dissolution with alkali extraction. Biotechnol. Bioeng. 109, 84-91. https://doi.org/10.1002/bit. 23281.

Government of Canada, 2017. Environmental Emergency Planning: Sodium Hydroxide Risk Evaluation [WWW Document]. URL. https://www.canada.ca/en/ environment-climate-change/services/environmental-emergencies-program/ regulations/sodium-hydroxide-risk-evaluation.html.
Gräsvik, J., Winestrand, S., Normark, M., Jönsson, L.J., Mikkola, J.P., 2014. Evaluation of four ionic liquids for pretreatment of lignocellulosic biomass. BMC Biotechnol. 14, 1-11. https://doi.org/10.1186/1472-6750-14-34.
Gupta, K.M., Jiang, J., 2015. Cellulose dissolution and regeneration in ionic liquids: a computational perspective. Chem. Eng. Sci. 121, 180-189. https://doi.org/10.1016/j.ces.2014.07.025.

Heinze, T., 2016. Cellulose chemistry and properties: fibers, nanocelluloses and advanced materials. In: Rojas, O.J. (Ed.), Advances in Polymer Science 271. Springer International Publishing Switzerland. https://doi.org/10.1007/978-3-319-26015-0. p. 341.

Hellenic Petroleum, 2013. Global Product Strategy (GPS) Safety Summary - Caustic Soda.
Imman, S., Arnthong, J., Burapatana, V., Champreda, V., 2015. Influence of alkaline catalyst addition on compressed liquid hot water pretreatment of rice straw. Chem. Eng. J. 278, 85-91. https://doi.org/10.1016/j.cej.2014.12.032.
Imman, S., Arnthong, J., Burapatana, V., Laosiripojana, N., Champreda, V., 2013. Autohydrolysis of tropical agricultural residues by compressed liquid hot water pretreatment. Appl. Biochem. Biotechnol. 170, 1982-1995. https://doi.org/10.1007/s12010-013-0320-1.
Imman, S., Laosiripojana, N., Champreda, V., 2018. Effects of liquid hot water pretreatment on enzymatic hydrolysis and physicochemical changes of corncobs. Appl. Biochem. Biotechnol. 1-12. https://doi.org/10.1007/s12010-017-2541-1.
Ioelovich, M., 2016. Isophase transitions of cellulose - a short review. Athens J. Sci. 3, 309-322. https://doi.org/10.30958/ajs.3-4-4.
Kamthai, S., Magaraphan, R., 2015. Thermal and mechanical properties of polylactic acid (PLA) and bagasse carboxymethyl cellulose (CMC B) composite by adding isosorbide diesters. AIP Conf. Proc. 1664. https://doi.org/10.1063/1.4918424.
Kawee-Ai, A., Srisuwun, A., Tantiwa, N., Nontaman, W., Boonchuay, P., Kuntiya, A., Chaiyaso, T., Seesuriyachan, P., 2016. Eco-friendly processing in enzymatic xylooligosaccharides production from corncob: influence of pretreatment with sonocatalytic-synergistic Fenton reaction and its antioxidant potentials. Ultrason. Sonochem. 31, 184-192. https://doi.org/10.1016/j.ultsonch.2015.12.018.
Kilpeläinen, I.L.K., Xie, H.A.X., King, A.L.K., Ranstrom, M.A.R.I.G., Eikkinen, S.A.M.I.H., Rgyropoulos, D.I.S.A., 2007. Dissolution of wood in ionic liquids. J. Agric. Food Chem. 9142-9148.
Kim, J.S., Lee, Y.Y., Kim, T.H., 2016. A review on alkaline pretreatment technology for bioconversion of lignocellulosic biomass. Bioresour. Technol. 199, 42-48. https://doi.org/10.1016/j.biortech.2015.08.085.
Kristensen, J.B., Thygesen, L.G., Felby, C., Jørgensen, H., Elder, T., 2008. Biotechnology for Biofuels Cell-wall structural changes in wheat straw pretreated for bioethanol production. Biotechnol. Biofuels 9, 1-9. https://doi.org/10.1186/1754-6834-1-5.
Lee, H.V., Hamid, S.B., Zain, S.K., 2014. Conversion of lignocellulosic biomass to nanocellulose : structure and chemical process conversion of lignocellulosic biomass to nanocellulose. Sci. World J. 2014, 1-14. https://doi.org/10.1155/2014/631013.

Li, M., Cao, S., Meng, X., Studer, M., Wyman, C.E., Ragauskas, A.J., Pu, Y., 2017. The effect of liquid hot water pretreatment on the chemical-structural alteration and the reduced recalcitrance in poplar. Biotechnol. Biofuels 10, 1-13. https://doi.org/10. 1186/s13068-017-0926-6.
Li, Y., Wang, J., Liu, X., Zhang, S., 2018. Towards a molecular understanding of cellulose dissolution in ionic liquids: anion/cation effect, synergistic mechanism and physicochemical aspects. Chem. Sci. 9, 4027-4043. https://doi.org/10.1039/C7SC05392D.
Liu, C., Li, B., Du, H., Lv, D., Zhang, Y., Yu, G., Mu, X., Peng, H., 2016. Properties of nanocellulose isolated from corncob residue using sulfuric acid, formic acid, oxidative and mechanical methods. Carbohydr. Polym. 151, 716-724. https://doi.org/10. 1016/j.carbpol.2016.06.025.
Lopes, J., Bermejo, M., Martín, Á., Cocero, M., 2017. Ionic liquid as reaction media for the production of cellulose-derived polymers from cellulosic biomass. ChemEngineering 1, 10. https://doi.org/10.3390/chemengineering1020010.
Luo, W., Wang, J., Liu, X., Li, H., Pan, H., Gu, Q., Yu, X., 2013. Bioresource Technology A facile and efficient pretreatment of corncob for bioproduction of butanol. Bioresour. Technol. 140, 86-89. https://doi.org/10.1016/j.biortech.2013.04.063.
Ma, Z., Pan, G., Xu, H., Huang, Y., Yang, Y., 2015. Cellulosic fibers with high aspect ratio from cornhusks via controlled swelling and alkaline penetration. Carbohydr. Polym. 124, 50-56. https://doi.org/10.1016/j.carbpol.2015.02.008.
Mahmood, H., Moniruzzaman, M., Yusup, S., Akil, H.M., 2016. Pretreatment of oil palm biomass with ionic liquids: a new approach for fabrication of green composite board. J. Clean. Prod. 126, 677-685. https://doi.org/10.1016/j.jclepro.2016.02.138.

Matsushima, J., Dowe, T.W., Arthaud, V.H., 1957. Evaluation of ground corncobs and corncob components as nutritive materials in rations for beef cattle. Historical Res. Bull. Nebraska Agric. Exp. Stn. 1913-1993.
Menard, K.P., 1999. Dynamic Mechanical Analysis - a Pratical Introduction, 1st ed. CRC Press LLC. CRC Press LLC, New York. https://doi.org/10.1201/9781420049183.ch2.
Michelin, M., Ruiz, H.A., Lourdes, M.De, Polizeli, T.M., Teixeira, J.A., 2018. Bioresource Technology Multi-step approach to add value to corncob: production of biomassdegrading enzymes, lignin and fermentable sugars. Bioresour. Technol. 247, 582-590. https://doi.org/10.1016/j.biortech.2017.09.128.
Michelin, M., Teixeira, J.A., 2016. Liquid hot water pretreatment of multi feedstocks and enzymatic hydrolysis of solids obtained thereof. Bioresour. Technol. 216, 862-869. https://doi.org/10.1016/j.biortech.2016.06.018.
Mtui, G.Y.S., 2009. Recent advances in pretreatment of lignocellulosic wastes and production of value added products. African J. Biotechnol. 8, 1398-1415. https://doi.org/10.1073/pnas.1014862107/-/DCSupplemental.www.pnas.org/cgi/.
Nabarlatz, D., Farriol, X., Montané, D., 2004. Kinetic modeling of the autohydrolysis of lignocellulosic biomass for the production of hemicellulose-derived oligosaccharides. Ind. Eng. Chem. Res. 43, 4124-4131. https://doi.org/10.1021/ie034238i.
Nor Amalini, A., Melina Cheah, M.Y., Wan Rosli, W.D., Hayati, S., Mohamad Haafiz, M.K., 2017. Fabrication and characterization of regenerated cellulose films obtained from oil palm empty fruit bunch. AIP Conf. Proc. 1901. https://doi.org/10.1063/1. 5010529.

Pang, J., Wu, M., Zhang, Q., Tan, X., Xu, F., Zhang, X., Sun, R., 2015. Comparison of physical properties of regenerated cellulose films fabricated with different cellulose feedstocks in ionic liquid. Carbohydr. Polym. 121, 71-78. https://doi.org/10.1016/j.carbpol.2014.11.067.

Pang, Z., Dong, C., Pan, X., 2016. Enhanced deconstruction and dissolution of lignocellulosic biomass in ionic liquid at high water content by lithium chloride.

Cellulose 23, 323-338. https://doi.org/10.1007/s10570-015-0832-7.
Park, S., Baker, J.O., Himmel, M.E., Parilla, P.A., Johnson, D.K., 2010. Cellulose crystallinity index: measurement techniques and their impact on interpreting cellulase performance. Biotechnol. Biofuels 3. https://doi.org/10.1186/1754-6834-3-10.
Pointner, M., Kuttner, P., Obrlik, T., Jäger, A., Kahr, H., 2014. Composition of corncobs as a substrate for fermentation of biofuels. Agron. Res. 12, 391-396.
Poletto, M., Pistor, V., Zattera, A.J., 2013. Structural characteristics and thermal properties of native cellulose. Cellul. Fundam. Asp 45-68. https://doi.org/10.5772/50452.

Porras, A., Maranon, A., 2012. Development and characterization of a laminate composite material from polylactic acid (PLA) and woven bamboo fabric. Compos. Part B Eng. 43, 2782-2788. https://doi.org/10.1016/j.compositesb.2012.04.039.
Qi, H., Chang, C., Zhang, L., 2009. Properties and applications of biodegradable transparent and photoluminescent cellulose films prepared via a green process. Green Chem. 11, 177-184. https://doi.org/10.1039/b814721c.
Rabemanolontsoa, H., Saka, S., 2016. Various pretreatments of lignocellulosics. Bioresour. Technol. 199, 83-91. https://doi.org/10.1016/j.biortech.2015.08.029.
Ravindran, R., Jaiswal, A.K., 2016. A comprehensive review on pre-treatment strategy for lignocellulosic food industry waste: challenges and opportunities. Bioresour. Technol. 199, 92-102. https://doi.org/10.1016/j.biortech.2015.07.106.
Reddy, J.P., Rhim, J.W., 2014. Isolation and characterization of cellulose nanocrystals from garlic skin. Mater. Lett. 129, 20-23. https://doi.org/10.1016/j.matlet.2014.05. 019.

Reddy, K.O., Maheswari, C.U., Dhlamini, M.S., Mothudi, B.M., Zhang, J., Zhang, J., Nagarajan, R., Rajulu, A.V., 2017. Preparation and characterization of regenerated cellulose films using borassus fruit fibers and an ionic liquid. Carbohydr. Polym. 160, 203-211. https://doi.org/10.1016/j.carbpol.2016.12.051.
Reddy, N., Yang, Y., 2005. Biofibers from agricultural byproducts for industrial applications. Trends Biotechnol. 23, 22-27. https://doi.org/10.1016/j.tibtech.2004.11.002.

Rhim, J.W., Reddy, J.P., Luo, X., 2015. Isolation of cellulose nanocrystals from onion skin and their utilization for the preparation of agar-based bio-nanocomposites films. Cellulose 22, 407-420. https://doi.org/10.1007/s10570-014-0517-7.
Sabanci, K., Buyukkileci, A.O., 2018. Bioresource Technology Comparison of liquid hot water, very dilute acid and alkali treatments for enhancing enzymatic digestibility of hazelnut tree pruning residues. Bioresour. Technol. 261, 158-165. https://doi.org/10.1016/j.biortech.2018.03.136.

Saldarriaga, J.F., Aguado, R., Pablos, A., Amutio, M., Olazar, M., Bilbao, J., 2015. Fast characterization of biomass fuels by thermogravimetric analysis (TGA). Fuel 140, 744-751. https://doi.org/10.1016/j.fuel.2014.10.024.
Sánchez, C., 2009. Lignocellulosic residues: biodegradation and bioconversion by fungi. Biotechnol. Adv. 27, 185-194. https://doi.org/10.1016/j.biotechadv.2008.11.001.
Segal, L., Creely, J.J., MartinJr, A.E., Conrad, C.M., 1959. An empirical method for estimating the degree of crystallinity of native cellulose using the X-Ray diffractometer. Têxtil Res. J. 29, 786-794. https://doi.org/10.1177/004051755902901003.
Seidl, P.R., Goulart, A.K., 2016. Pretreatment processes for lignocellulosic biomass

conversion to biofuels and bioproducts. Curr. Opin. Green Sustain. Chem. 2, 48-53. https://doi.org/10.1016/j.cogsc.2016.09.003.
Silva, J.Cda, Oliveira, R.Cde, Neto, Ada S., Pimentel, V.C., Santos, A., dos, de A., 2015. Extraction, addition and characterization of hemicelluloses from corn cobs to development of paper properties. Procedia Mater. Sci. 8, 793-801. https://doi.org/10.1016/j.mspro.2015.04.137.
Silvério, H.A., Flauzino Neto, W.P., Dantas, N.O., Pasquini, D., 2013. Extraction and characterization of cellulose nanocrystals from corncob for application as reinforcing agent in nanocomposites. Ind. Crops Prod. 44, 427-436. https://doi.org/10.1016/j.indcrop.2012.10.014.
Singh, R., Krishna, B.B., Kumar, J., Bhaskar, T., 2016. Opportunities for utilization of nonconventional energy sources for biomass pretreatment. Bioresour. Technol. 199, 398-407. https://doi.org/10.1016/j.biortech.2015.08.117.
Singh, S., Varanasi, P., Singh, P., Adams, P.D., Auer, M., Simmons, B.A., 2013. Understanding the impact of ionic liquid pretreatment on cellulose and lignin via thermochemical analysis. Biomass Bioenergy 54, 276-283. https://doi.org/10.1016/j.biombioe.2013.02.035.

Sun, Y., Cheng, J., 2002. Hydrolysis of lignocellulosic materials for ethanol production : a review q. Bioresour. Technol. 83, 1-11. https://doi.org/10.1016/S0960-8524(01) 00212-7.
Swatloski, R.P., Spear, S.K., Holbrey, J.D., Rogers, R.D., 2002. Dissolution of cellulose with ionic liquids. J. Am. Chem. Soc. 124, 4974-4975 https://doi.org/ja025790m.
Teng, H., Lin, H.C., Ho, J.A., 1997. Thermogravimetric analysis on global mass loss kinetics of rice hull pyrolysis. Ind. Eng. Chem. Res. 36, 3974-3977. https://doi.org/10.1021/ie970017z.

Thangavelu, K., Desikan, R., Taran, O.P., Uthandi, S., 2018. Biotechnology for Biofuels Delignification of corncob via combined hydrodynamic cavitation and enzymatic pretreatment : process optimization by response surface methodology. Biotechnol. Biofuels 1-13. https://doi.org/10.1186/s13068-018-1204-y.
Thygesen, A., Oddershede, J., Lilholt, H., Thomsen, A.B., Ståhl, K., 2005. On the determination of crystallinity and cellulose content in plant fibres. Cellulose 12, 563-576. https://doi.org/10.1007/s10570-005-9001-8.
Ullah, K., Kumar Sharma, V., Dhingra, S., Braccio, G., Ahmad, M., Sofia, S., 2015. Assessing the lignocellulosic biomass resources potential in developing countries: a critical review. Renew. Sustain. Energy Rev. 51, 682-698. https://doi.org/10.1016/j.rser.2015.06.044.
Upajak, S., Laosiripojana, N., Champreda, V., Kreethachart, T., Thonburi, T., Author, C., 2018. Effect of combination of liquid hot water system and hydrogen peroxide pretreatment on enzymatic. Int. J. GEOMATE 15, 31-38.
Wan, C., Zhou, Y., Li, Y., 2011. Bioresource Technology Liquid hot water and alkaline pretreatment of soybean straw for improving cellulose digestibility. Bioresour. Technol. 102, 6254-6259. https://doi.org/10.1016/j.biortech.2011.02.075.
Wan Daud, W.R., Djuned, F.M., 2015. Cellulose acetate from oil palm empty fruit bunch via a one step heterogeneous acetylation. Carbohydr. Polym. 132, 252-260. https://doi.org/10.1016/j.carbpol.2015.06.011.
Wang, F., Li, S., Sun, Y., Han, H., Zhang, B., 2017. Ionic liquids as e ffi cient pretreatment solvents for lignocellulosic biomass. R. Soc. Chem. 7, 47990-47998. https://doi.org/10.1039/c7ra08110c.

Wang, S., Lu, A., Zhang, L., 2016. Recent advances in regenerated cellulose materials. Prog. Polym. Sci. 53, 169-206. https://doi.org/10.1016/j.progpolymsci.2015.07. 003.

Wulandari, W.T., Rochiliadi, A., Arcana, I.M., 2016. Nanocellulose prepared by acid hydrolysis of isolated cellulose from sugarcane bagasse. Mater. Sci. Eng. 1-8. https://doi.org/10.1088/1757-899X/107/1/012045.
Xie, N.A.N., Jiang, N., Zhang, M., Al, E., 2014. Cellulose chemistry and technology effect of different pretreatment methods of corncob on bioethanol production and enzyme recovery. Cellul. Chem. Technol. 48, 313-319.
Yang, H., Shi, Z., Xu, G., Qin, Y., Deng, J., Yang, J., 2019. Bioresource Technology Bioethanol production from bamboo with alkali-catalyzed liquid hot water pretreatment. Bioresour. Technol. 274, 261-266. https://doi.org/10.1016/j.biortech. 2018.11.088.

Yeng, L.C., Wahit, M.U., Othman, N., 2015. Thermal and flexural properties of regenerated cellulose(RC)/poly(3- hydroxybutyrate)(PHB)biocomposites. J. Teknol. 75, 107-112. https://doi.org/10.11113/jt.v75.5338.
Yu, L., Lin, J., Tian, F., Al, E., 2014. Cellulose nanofibrils generated from jute fibers with tunable polymorphs and crystallinity. J. Mater. Chem. A 6402-6411. https://doi.org/10.1039/c4ta00004h.

Yu, Q., Zhuang, X., Lv, S., He, M., Zhang, Y., Yuan, Z., Qi, W., Wang, Q., Wang, W., Tan, X., 2013. Bioresource Technology Liquid hot water pretreatment of sugarcane bagasse and its comparison with chemical pretreatment methods for the sugar recovery and structural changes. Bioresour. Technol. 129, 592-598. https://doi.org/10.1016/j.biortech.2012.11.099.

Yue, Y., Han, J., Han, G., Aita, G.M., Wu, Q., 2015. Cellulose fibers isolated from energycane bagasse using alkaline and sodium chlorite treatments: structural, chemical and thermal properties. Ind. Crops Prod. 76, 355-363. https://doi.org/10.1016/j. indcrop. 2015.07.006.
Zhang, J., Feng, L., Wang, D., Zhang, R., Liu, G., Cheng, G., 2014. Thermogravimetric analysis of lignocellulosic biomass with ionic liquid pretreatment. Bioresour. Technol. 153, 379-382. https://doi.org/10.1016/j.biortech.2013.12.004.
Zhang, K., Xiao, H., Su, Y., Wu, Y., Cui, Y., Li, M., 2019. Mechanical and physical properties of regenerated biomass composite films from lignocellulosic materials in ionic liquid. BioResources 14, 2584-2595.
Zhang, Q., Hu, J., Lee, D.J., 2017. Pretreatment of biomass using ionic liquids: research updates. Renew. Energy 111, 77-84. https://doi.org/10.1016/j.renene.2017.03.093.
Zhang, X., Xiao, N., Wang, H., Liu, C., Pan, X., 2018. Preparation and characterization of regenerated cellulose film from a solution in lithium bromide molten salt hydrate. Polymers (Basel) 8. https://doi.org/10.3390/polym10060614.
Zhang, X.Q., Chen, M.J., Wang, H.H., Wen, X.X., Liu, C.F., Sun, R.C., 2016. Ionic liquid as green solvent for ring-opening graft polymerizaion of ε-caprolactone onto hemicelluloses. In: Handy, S. (Ed.), Ionic Liquids: Current State of the Art. IntechOpen, pp. 13. https://doi.org/10.5772/57353.

Zhou, Z., Lei, F., Li, P., Jiang, J., 2018. Lignocellulosic biomass to biofuels and biochemicals: a comprehensive review with a focus on ethanol organosolv pretreatment technology. Biotechnol. Bioeng. 115, 2683-2702. https://doi.org/10.1002/bit. 26788.